CoA NOTE MAT. No. 18

THE COLLEGE OF AERONAUTICS

CRANFIELD

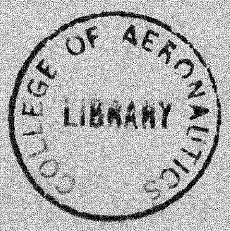

THE DESIGN AND CONSTRUCTION OF A WELD HEAT-AFFECTED ZONE SIMULATOR

by

T. E. Clifton and M. J. George

CoA Note Mat. No. 18

February, 1968

THE COLLEGE OF AERONAUTICS

DEPARTMENT OF MATERIALS

The design and construction of a weld heat-affected zone simulator

- by -

T.E. Clifton and M.J. George

SUMMARY

Investigation of the structure and properties of the heat-affected zones in welded joints is usually limited by their small size and their complexity. One method of overcoming this problem is to simulate the structure at a particular point in the heat-affected zone in a specimen of larger size by imposing on it the thermal cycle sustained at that point.

The equipment described in this note uses a.c. resistance heating and water cooling to impose thermal cycles on 2.5" x 0.4" x 0.4" specimens, the thermal cycle being chosen by adjustment of a bank of variable resistors to construct a voltage analogue. Control of specimen temperature is achieved using a thyristor and two ignitrons to control the input at 440V. to a welding transformer. Feedback is applied from a thermocouple welded to the specimen hot-zone. The equipment has been shown to produce the desired thermal cycles in a reproducible manner.

Contents

Introduction

As welding techniques become more and more refined, and welded structures are put into service in applications which demand increasing degrees of reliability e.g. natural gas pipelines, nuclear engineering, it is important that all possible techniques should be used to increase our understanding of the factors underlying satisfactory welded-joint performance.

A welded joint contains zones which have had widely differing thermal histories, and which may show, therefore, very different mechanical properties. Three major zones exist:-

i) The weld metal, which has been in the molten state, and which shows the general characteristics of cast material;

ii) The parent material, with microstructure and properties totally unaffected by the heating sustained during welding;

iii) The heat-affected zone, which lies between the fusion boundary on one side and the unaffected parent metal on the other. Figure 1 shows these zones in a section taken through a butt-weld.

The heat-affected zone material generally forms a very small part of a welded structure as a whole, but may decide the overall performance of the structure, on a 'weakest-link' basis. Many welded structures have failed, usually with expensive results, because of the effect of the welding process on the immediately adjacent material i.e. the heat-affected zone, which led to a local reduction in ductility and fracture toughness, and allowed easy propagation of fractures originating at some welding or material defect. For this reason, the integrity of an entire welded structure may depend on the production, in the HAZ, of satisfactory mechanical properties by controlling the microstructure. In order to do this, however, one must know:-

a) the structure and properties of the HAZ in a particular material, and

b) which structures will be unacceptable, and how they may be modified, for instance, by weld pre-heat or post-heat treatment

Much of the investigational work on the common structural steels is of an ad-hoc nature, designed either to establish a satisfactory welding procedure or to solve some particular fabrication problem, and there is a need for longer-term investigations into the behaviour of even the best-known structural steels, to gain an understanding of the heat-affected zones.

However the heat-affected zones are usually only of the order of millimetres in width, and are completely inhomogeneous in nature, since the thermal cycles sustained change continually across the width of the heat-affected zone. For these reasons, it is not feasible to cut test-pieces for the usual

mechanical tests directly from a HAZ, although hardness surveys are frequently carried out, and notch toughness specimens have been cut transversely from welded joints. Notches placed at increasing distances from the weld fusion boundary give information on changes in impact toughness across the HAZ (1). However, these techniques are of limited value.

Alternatively, we can aim to produce, in specimens large enough to allow conventional mechanical testing, equivalent microstructures, and hence mechanical properties, to those obtaining at specific positions inside the HAZ, by imposing the same thermal cycles sustained during welding. This note describes the design and construction of equipment to carry out such simulation.

Figure 2 shows the thermal cycles sustained at various distances from the fusion boundary in a weld of 77,000 J/in. heat input in $^{3}/_{4}$" thick plate, with no pre-heat. The cycles were obtained by means of thermocouples flash-welded into position prior to welding. The main feature is a rapid rise to a peak temperature, which is a function of distance from the fusion boundary, followed by cooling to room temperature at an exponentially declining rate. In considering the visible HAZ in steels, as shown in Figure 1, we are concerned with peak temperatures in the approximate range 700°-1500°C. However, there appears to exist, outside the visible HAZ, a region of low ductility in which thermal stressing beyond the yield point, at temperatures of around 100°-300°C, has produced strain ageing (2), and which should properly be included within the term 'heat-affected zone'.

The peak temperature achieved, and the rates of heating and cooling, vary widely in welding as a whole, and are controlled by such process variables as the type of welding process used, the heat input per inch of weld, the plate thickness and the degree of pre-heat used. In addition, there is a rapid drop in peak temperature and heating and cooling rates, as the distance from the fusion boundary increases (Figure 3).

The properties of the HAZ produced by a weld run are affected by the heating from subsequent runs, in a multi-run weld, and by any post-weld heat-treatment. In general, the effects of both of these are beneficial.

The general principles of the design

In order to impose thermal cycles of the type shown in Figure 2, the prime requirement was the supply and abstraction of large amounts of heat to the specimen, in a short time and in a controlled fashion.

Two possible methods of heating were high frequency induction heating and resistance heating. Induction heating at the necessary rates would be difficult, and the well-known h/f skin-heating effect could produce inhomogeneous temperature distributions within the specimen. In addition, the capital cost of heating equipment would be relatively high. Nevertheless, h/f induction heating was used for at least one HAZ simulator (5).

D.C. resistance heating would be ideal in providing uniform heating at the necessary rates but the provision of the necessary power at low impedance is a considerable problem. A.C. resistance heating, using a welding transformer as an impedance converter, is a ready source of the necessary power, although it has the drawbacks of skin-heating effects, the severity of which varies with temperature and heating rates, and the possibility of interference, produced by the large a.c. fields, in the operation of external circuits, necessitating shielding precautions. However, low frequency a.c. heating has been used with success in developing other HAZ simulators (6,7) and this technique was chosen for the present work.

Cooling was achieved by circulating water, at full mains pressure, through copper specimen grips, ensuring that the natural cooling rate, i.e. in the absence of any heating, was in excess of those necessary for simulation of the required thermal cycles, so that control of the cooling rate could be maintained by a variable amount of heat input to the specimen during cooling.

The general design requirements were:-

i) a heat input variable over a wide range during the cycle;

ii) accurate control of heating and cooling rates;

iii) maximum reproducibility between successive runs at a given setting of the controls;

iv) easy variation of the demand cycle, with a minimum of readjustment;

v) a record of the temperature cycle imposed on each specimen, as a check on accuracy and reproducibility of the thermal cycle.

The specimen is 0.4" square by 2.5" long, large enough to allow a Charpy impact specimen or a small tensile specimen to be machined from it, after heat-treatment. The heat-treated volume is approximately a 0.4" cube in the specimen centre. Heating and cooling rates were more likely to be uniform in a cube-shaped element.

3. The specimen grips

The specimen grips consist of four 2" x 2" x $1\frac{5}{8}$" copper blocks, through which water is circulated at full mains pressure. Each end of the specimen is gripped between two blocks by means of four 5/16" bolts (Figure 4). In early trials, it was found that the resistance across the specimen grips affected the peak temperature achieved at a given control setting, giving poor specimen-to-specimen reproducibility. To standardize resistance as far as possible, soft aluminium packing pieces are used on each face of the specimen in contact with a copper block, and the bolts are tightened to 50 lbs-ins. by means of a torque wrench.

The copper blocks are mounted on a $1\frac{5}{8}$" thick Tufnol block, backed with $\frac{5}{8}$" steel plate to restrain the thermal expansion of the specimen during cycling.

This approximates, to some extent, at least, to the restraint on the HAZ in an actual weld joint.

Connections to the transformer were made as short and thick as possible ($1\frac{1}{2}$" x 1" x 5" long) to minimise the voltage drop. The voltage across the transformer output terminals is 4V. approx. and across the specimen grips 1.5 V. approx. Current taken during the heating portion of the cycle may be as high as 15,000 A.

A modification to this arrangement was made during work on the effect of variation in restraint (4), in which one end of the specimen was allowed to move during expansion and contraction. One pair of blocks was mounted on a ball-bearing slide and the power fed in via flexible connections.

4. The control circuit

Basically, the control circuit continually compares the specimen temperature, measured by a thermocouple, with the required thermal cycle, as given by a function generator. The polarised error signal thus obtained is used to control the heat input to the specimen.

This control circuit may be considered in two sections:-

a) The function generator and comparison network

It was necessary to generate a voltage analogue of the required temperature cycle, which was then compared continuously with the e.m.f. produced by the thermocouple attached to the specimen, i.e. with the specimen temperature. As the development of the simulator progressed, this was achieved in three different ways.

Originally, a cam, obtained by plotting the chosen experimental time-temperature curve in a polar fashion, was rotated through 360°C, at the correct constant speed. By connecting a cam follower to the wiper of a 10 KΩ linear potentiometer and using a suitable voltage supply across the potentiometer, a voltage-time relationship matching the desired temperature-time curve was produced. Owing to mechanical problems, such as backlash, and the labour of constructing the large number of cams required, this method was eventually superseded. Correction of errors occurring in cycles with rapid heating rates (discussed later) required on-the-spot 'trial and error' modifications of the cam shape, and this difficulty contributed to the decision to discard this method. However, the cam unit served satisfactorily as the function generator during one programme of research (4).

It was replaced by a simpler function generator, in which a single-turn potentiometer with 34 taps, equally spaced over its resistance range, was driven at a constant speed over its 340°C arc. The potentiometer (A) is shown with the driving motor (B), in Figure 5. A variable resistor was connected in series with the potentiometer and a stabilised d.c. potential connected as shown in Figure 8. By adjusting the tap to which the positive voltage

connection to the network is made, and by adjusting the value of the series resistor, the shape of the output function can be varied with respect to the proportion of the cycle time occupied in rising to the peak, and the magnitude of the final output voltage, respectively. Further, by modifying the total resistance value at each tap position, by suitable parallel fixed-value resistors, the voltage-time function can be modified to produce a shape equivalent to that of the required experimental curve. Although this is constructed from a series of straight lines between adjacent tap positions, a very satisfactory approximation is obtained. The method used to calculate the values of the parallel resistors is shown in the Appendix.

The major drawback was in the selection of suitable fixed value resistors, together with the labour of constructing a resistor bank for each demand cycle required. Adjustment of errors produced by high heating and cooling rates, as before, was also difficult. Accordingly, the equipment in its latest form, on the right of Figure 6, contains a bank of multi-turn potentiometers connected in parallel with the segments of the function generator potentiometer. During the latter part of the cycle, the slope of the required function is generally small, requiring parallel resistors of low value. For this reason, several of the parallel potentiometers span two segments towards the end of the cycle. A diagram showing the lay-out of the parallel potentiometers, giving their values and span is given in the Appendix. Sockets have been provided to enable fixed value resistors to be connected in series with the first six helical potentiometers, when the calculated resistance is outside the range of the potentiometer.

Taps 2 to 7 are connected to the supply positive through a single pole six-way switch (C in Figure 5) which allows the peak position to be selected. In addition, the rotational speed of the function generator can be adjusted, allowing the setting-up of a wide variety of cycles on the single apparatus.

The voltage analogous to the specimen temperature, i.e. the feedback signal required to close the loop, is obtained by amplifying the voltage output from a fine Chromel-Alumel thermocouple, capacitor-discharge welded on to the centre of the heated zone of the specimen.

The thermocouple output is connected into a single channel Graphispot recorder, shown on the left in Figure 6, which, as well as producing a record of the temperature cycle sustained by the specimen, gives an output voltage proportional to the pen displacement. This is achieved by using a 10 KΩ linear potentiometer mechanically connected across the scale of the instrument, with the wiper connected to the pen carriage. The voltage across the potentiometer is provided externally, and can be varied as required, providing a high-gain d.c. amplifier for the thermocouple e.m.f.

The supply voltages across the function generator and Graphispot potentiometers are chosen to give error voltages of the correct magnitude to feed directly into the heat control unit, and thus are a means of controlling the sensitivity of the heating circuit to deviations from the required temperature.

b) The heat-control unit

The heat-control unit was designed to accept signal voltages between zero volts (maximum power) and +10 volts (minimum power). As the error signal approaches zero, the demand will be for decreasing power, therefore a datum shift, provided by a suitably-polarised fixed-value d.c. voltage, is required.

The unit was originally supplied as a modification of a commercial spot-welder control unit, but after unsatisfactory performance and frequent component failure, it was redesigned by the Instrumentation Section of Electrical Department, for whose help we are most grateful. The unit is now performing satisfactorily.

As the method used in controlling the power to the primary of the welding transformer is relevant to many control problems encountered in welding techniques, the type of circuit employed will be described more fully. A circuit diagram showing details of the heat control unit is shown in Figure 9.

A 12 volt r.m.s. voltage in phase with the ignition supply is full-wave rectified to give, via a pulse forming network, comprising transistor T_1 and associated components, a pulse of 100 c.p.s. on the base of transistor T_3. Transistor T_2 is a constant current generator charging the 0.47 μF capacitor to give a voltage ramp dependent upon the time constant of the network. The current is turned on with the initiation contacts closed. Normally, T_1 is turned on, cutting off T_3, so that at the beginning of each half-cycle, the action of T_1 and T_3 is to discharge the capacitor. Therefore, a ramp is produced which is reset at the beginning of each half-cycle. This ramp is applied, via an emitter follower to a Schmitt trigger network whose hold off bias is a function of the control signal.

By this means the trigger is made to operate at a time after the beginning of each $\frac{1}{2}$ cycle depending upon the value of the control voltage. The Schmitt trigger pulse fires a blocking oscillator, which produces the necessary firing pulse for the thyristor.

440 volts is connected, via the routing diodes D_1, D_2, D_3 and D_4, to the appropriate ignitron ignitor, through the single thyristor, the magnitude of the r.m.s. current to the transformer primary being determined by the time delay, as set by the d.c. control voltage (error signal). The function of the Zener diode, in series with the thyristor, is to ensure that the thyristor current goes to zero, and thus extinguishes, at the end of each half-cycle. This is necessary because of the inductive nature of the load, which produces phase shift between load current and voltage, and would normally prevent extinction after each half-cycle. The capacitor-resistor combination in parallel with the thyristor is designed as a transient filter, to prevent spurious voltage spikes from firing the device.

The power supply to the mains transformer is therefore controlled by two ignitrons, connected back-to-back, so that each fires on successive half-cycles

of the supply voltage. The action of the heat-control unit is to vary the proportion of each half-cycle over which the ignitrons will fire, as the signal voltage varies in the range 0 to 10V.

The temperature control of the specimen is therefore basically proportional in character, since the amount of power applied is a direct function of the deviation of the specimen temperature from the instantaneous demand value. Because of the complex feedback loop, there is a tendency to introduce a time-lag into the response of the system. Further, since the desired temperature is constantly changing the effect of a time-lag is to distort the thermal cycle imposed on the specimen. Since the lag is greatest at high heating rates, the effects are seen most in the peak temperature region. The parameters of the cycle most affected are the rate of heating, which will be higher than that required, and the peak temperature, which will be exceeded. This effect is partially overcome by altering the voltage across the Graphispot and function-generator potentiometers until the peak temperature is achieved. Since the time-lag varies throughout the cycle with change in heating and cooling rates, the voltage adjustment which gives the correct peak temperature gives an error elsewhere, notably a droop in the curve at lower temperatures towards the end of the cycle. When cams were used, this was corrected by modifying the appropriate section by filing and in the later versions, using the series variable resistor to give the correct voltage at the end of the cycle. This can be simplified by adding a derivative control term to the basic proportional term, to give an automatic correction of the signal voltage, with a maximum effect at high heating rates and a minimum at the lower rates towards the end of cycle. It was found, however, that the magnitude of the derivative component required to achieve control of the initial heating rate was so large as to introduce instability in the degree of control elsewhere in the cycle, particularly very near to the peak position, where the derivative component is removed very rapidly, producing an over-reaction of the control system and a double-peak effect on the specimen thermal cycle.

Ad-hoc modification of the shape of the thermal cycle, by altering the parallel resistor values, achieves the same result in a relatively short time, and this method of adjusting the shape of the thermal cycle proved a viable proposition, in practice.

5. Assessment of simulator performance

i) Heat control unit

The modified heat control unit operated very satisfactorily during the test period. Adjustment of the heating rate during the cycle occurred smoothly and there was a general lack of any random firing by mains transients which was a too-frequent occurrence with the original unit.

ii) Accuracy of Control

This was difficult to assess quantitatively during a continuously changing demand cycle, but on a qualitative basis, the degree of control appeared to be

sufficient, where a true control situation applied, e.g. if the potentiometer drive motor was halted during the cooling period, the specimen was held at a constant temperature, with no noticeable fluctuation on the Graphispot record. The response of the control circuit is adjustable by variation of the voltages across the function generator and Graphispot potentiometers, and an optimum range of values lies just below voltages at which over-reaction occurs, giving 'hunting' of the temperature.

If true control could be achieved at all points on the thermal cycle, as would be the case with slow heating rates, the voltages across the function generator and Graphispot potentiometers would be approximately equal. With the heating rates encountered in the cycles shown in Figure 2, up to around 600°C/second, a small time-lag built up in the peak temperature region, giving a peak temperature higher than the required value. Correction was applied by making the voltage across the function generator lower than that across the Graphispot potentiometer. This then introduced distortion in the latter part of the curve, where true control was achieved.

iii) Reproducibility

Successive demand cycles were found to be essentially identical. Specimen-to-specimen fluctuations of the thermal cycle produced did, however, occur, although these were felt to be due more to such factors as inconsistencies in specimen set-up or in mains voltage, rather than to deficiency of any part of the control circuit.

Heating, particularly in the early stages, was observed to occur mainly due to interfacial heating,which could obviously vary from one specimen to the next, affecting the efficiency of heating during the critical and least-controlled seconds leading up to the peak value. Aluminium packing pieces were necessary to give even electrical contact between the specimen and the water cooled blocks, in order to prevent sparking during periods of high heating rates. To standardise, as far as possible, inter-facial conditions, fresh packing pieces were used for each specimen, and the clamping nuts tightened evenly and to a constant 50 lb.in. torque, using a torque wrench.

Applying these precautions, it was possible to produce sets of specimens with essentially identical thermal cycles. For instance, 24 specimens were produced having had the 940°C peak temperature cycle, with peak temperatures lying within ± 25°C of 940°C. Twelve specimens in which the peak temperatures all lay within ± 10°C of that required, i.e. within an error of ± 1% were selected for Charpy impact testing.

Because of the large scatter in the Charpy test, it was most important that, as near as was possible, the specimens were identical. The specimens with less accurate cycles were kept for less demanding uses, such as tensile testing and metallography.

iv) Variation of demand cycle

The values of parallel resistance required to produce a resistance

analogue of the desired cycle can be calculated, using the method given in the Appendix. Since velocity feedback proved impractible, the distortion produced with fast heating rates was corrected by trial-and-error modification of the parallel resistors in the distorted region. This modification was akin to the modification of cam shapes which was necessary when the driven-cam function generator was in use (4), but was much easier to carry out. Depending on the degree and extent of distortion present, 1 - 2 hours was sufficient to give a satisfactory fit to the experimental curve. A subsequent specimen production rate of about 10 minutes per specimen enables a set of 24 specimens to be produced in 1 - $1\frac{1}{2}$ working days, thus providing the raw material for a considerably longer period of further work. Specimen-production time is, therefore, a relatively small fraction of the total time of a research programme. Figures 10, 11 and 12 show the three uppermost curves of Figure 2, together with the simulated thermal cycles.

6. Further applications of the simulator

Because of the high heating and cooling rates available, the close temperature control, and the ability to programme a heat treatment cycle, the simulator can be used quite generally as a heat-treatment facility. In particular heat-treatments requiring continuous or discontinuous variation of temperature are easily and quickly carried out, making it a very useful research tool.. During long heating periods, decarburisation and oxidation are likely to occur. The enclosure of the specimen grips in a vacuum chamber, allowing treatment in vacuo or under controlled atmosphere, is a possible further development.

With suitable modification of the specimen grips, other techniques which might be employed are, a) high speed dilatometry, to ascertain the true transformation temperatures applying to the heating and cooling rates encountered in HAZ thermal cycles, and b) tensile testing at high temperatures.

Appendix

Calculation of resistance analogue

Figure A1 represents the function generator (tapped potentiometer) without the parallel resistors.

With $E_1 = E_2$

With wiper B at A

$$E_3 = 0$$

With wiper B at T_2 and wiper X at T_2

$$E_3 = E_1 = E_2$$

With wiper B at C and wiper X at T_2

$$E_3 = E_1 - E_2 \left(T_2.C/T_2D\right)$$ (T_2C represents total resistance between point T_2 and C).

Figure A2 shows a series of curves representing output voltage E_3 plotted against wiper B position, for different connections of wiper X. A similar graph may be constructed with resistance between A and B, figure A1, replacing voltage on the Y axis. Then by modifying the resistance value at tap positions, throughout the whole range of the potentiometer, a curve of the desired shape can be constructed. The curve will be constructed from a series of straight lines between adjacent tap positions, as shown in Figure A3.

The position chosen for wiper X (Figure A1) will depend upon the shape of the thermal cycle required.

As a general rule, for slow heating rates a high tap position should be selected, and for high heating rates, a low tap position is more advantageous.

Figure 3 shows that for slow heating rates, especially when the heating curve deviates markedly from a straight line, a greater number of segments are needed to simulate closely the desired function.

The speed of rotation of the function generator should be selected to satisfy the following conditions:

(a) The peak of the resistance curve should fall as nearly as possible to a tap position, (especially important for high heating rates),

(b) The time for a complete revolution should correspond to the cycle time for the thermal cycle required.

Having selected a position of wiper X and the cycle time of the function generator, the experimental temperature cycle should be plotted to the above

time base, marking on the X axis the positions of the potentiometers taps.

The Y axis is then converted from thermocouple output to resistance, using a peak value of between 700 and 800Ω, and evaluate the resistance at tap positions.

The resistance of the function generator potentiometer is 20KΩ which gives a resistance of 590Ω between adjacent taps. For the majority of experimental curves a peak value of 700 - 800Ω gives parallel resistances which are real, and fall within the range of the helical potentiometers fitted.

Figure A4 is a typical temperature time curve, and the procedure for calculation of parallel resistance values is detailed below.

The position of the X wiper in the example was chosen for tap 3, with the peak temperature converted to 800Ω.

The resistance at tap 1 must total 410Ω.

i.e. 590Ω in parallel with resistor R_1, must equal 410Ω

$$\frac{590R_1}{590+R_1} = 410 \quad R_1 \simeq 1340\Omega$$

The resistance at tap 2 must total 700Ω

i.e. 590Ω in parallel with resistor R_2 in series with 410Ω must equal 700Ω

$$410 + \frac{590R_2}{590+R_2} = 700 \quad R_2 \simeq 570\Omega$$

Similarly the resistance at tap 3 must total 800Ω

$$700 + \frac{590R_3}{590+R_2} = 800 \quad R_3 \simeq 120\Omega$$

Continuing from the peak tap position the procedure is somewhat modified.

The peak is called zero, the curve is inverted (Voltage E_2 opposes E_1) and the parallel resistance calculated as before.

Figure A5 shows the inverted curve of the example shown in Figure A4

The resistance at tap 4 must total 60Ω (i.e. 800-740)

$$\frac{590R_4}{590+R_4} = 60 \quad R_4 \simeq 66.9\Omega$$

Similarly the resistance at tap 5 must total 220Ω (800-580)

$$60 + \frac{590R_5}{590+R_5} = 220 \quad R_5 \simeq 219\Omega$$

and so on.

The value of the series resistor (CD in fig. A1) is calculated as follows.

Total value of resistance from peak position to finish must equal the value from peak to start, which is, in the example considered, 800Ω.

Therefore: Value of series resistor = 800 - value at final tap.

The table shows the value of each parallel helical potentiometer and the relevant tap position. Each potentiometer requires 10 complete revolutions to scan the total range and the turns indicator fitted shows the precise position of the wiper.

Figure A6 shows the potentiometer layout on the front panel.

Towards the end of the cooling curve, where the slope is small, parallel resistors have been connected to span, in some cases, two segments.

This must be taken into consideration in the calculations.

The fixed value will, in these cases, be 1180Ω instead of 590Ω.

Acknowledgements

The authors wish to thank E. Sills and B. Moffat of the Instrumentation Section for advice and practical assistance in the redesign of the heat control unit, and T. Biston of the Department of Materials, for carrying out the construction of the simulator.

References

1. A.C. de Koning — I.I.W. Document IX-471-65

2. C.F. Tipper — Brit. Weld. J., 1966, 13, p. 461-466.

3. M.J. George — Unpublished work, Cranfield, 1966.

4. M.D. Coward — M.Sc. Thesis, London University, 1967.

5. M. Inagaki et al. — Trans. Nat. Res. Inst. Met. (Japan), 1964, 6, p. 39.

6. E.F. Nippes and W.F. Savage — Weld. J., 1949, 28, p. 534s.

7. E. Fletcher and D. Shaw — Swinden Laboratories, United Steel Co's. Ltd., 1961. (Private Communication).

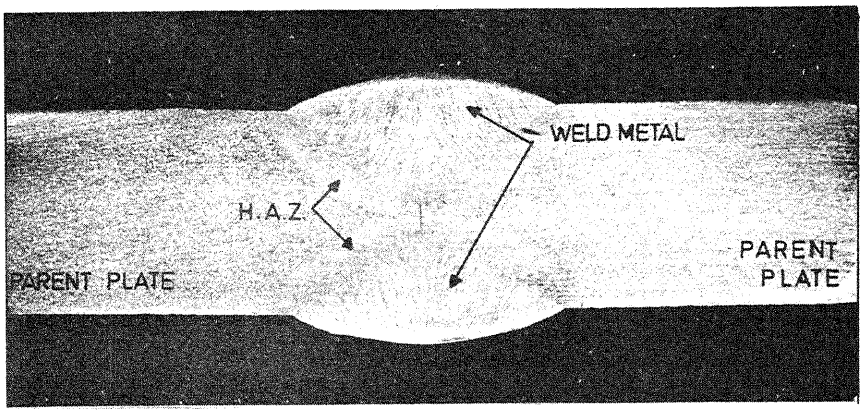

FIG. 1. MACROGRAPH OF BUTT WELD SHOWING POSITION OF HEAT AFFECTED ZONES (x 2 MAGNIFICATION).

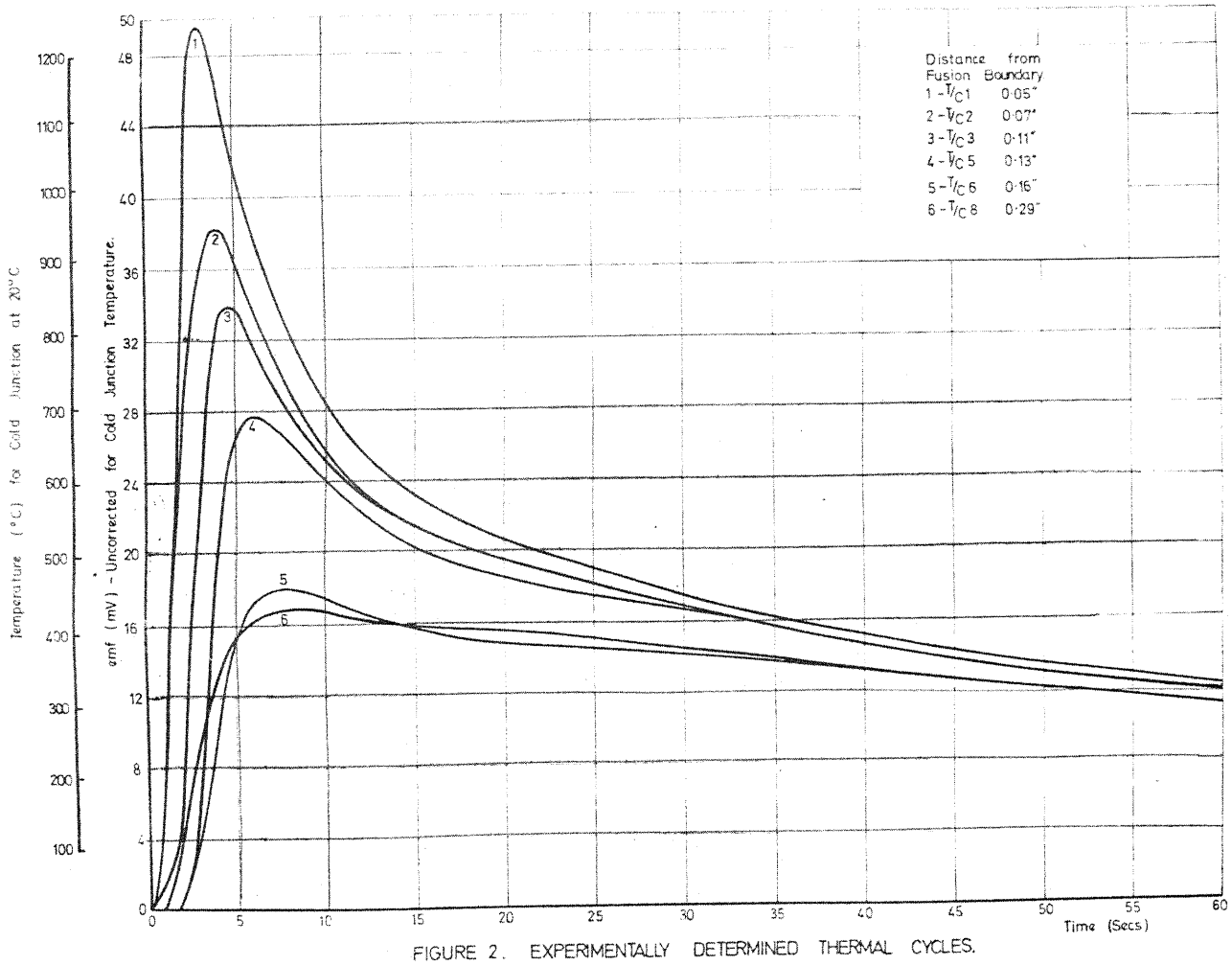

FIGURE 2. EXPERIMENTALLY DETERMINED THERMAL CYCLES.

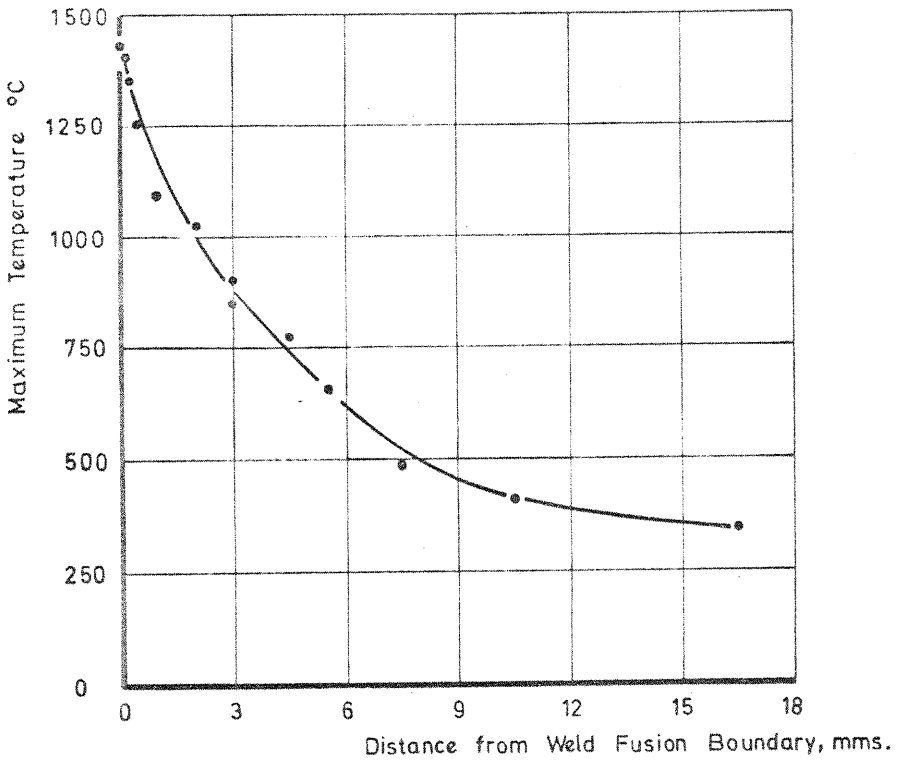

FIG. 3 RELATIONSHIP BETWEEN PEAK TEMPERATURE AND THE DISTANCE FROM THE FUSION BOUNDARY, REFERENCE 4

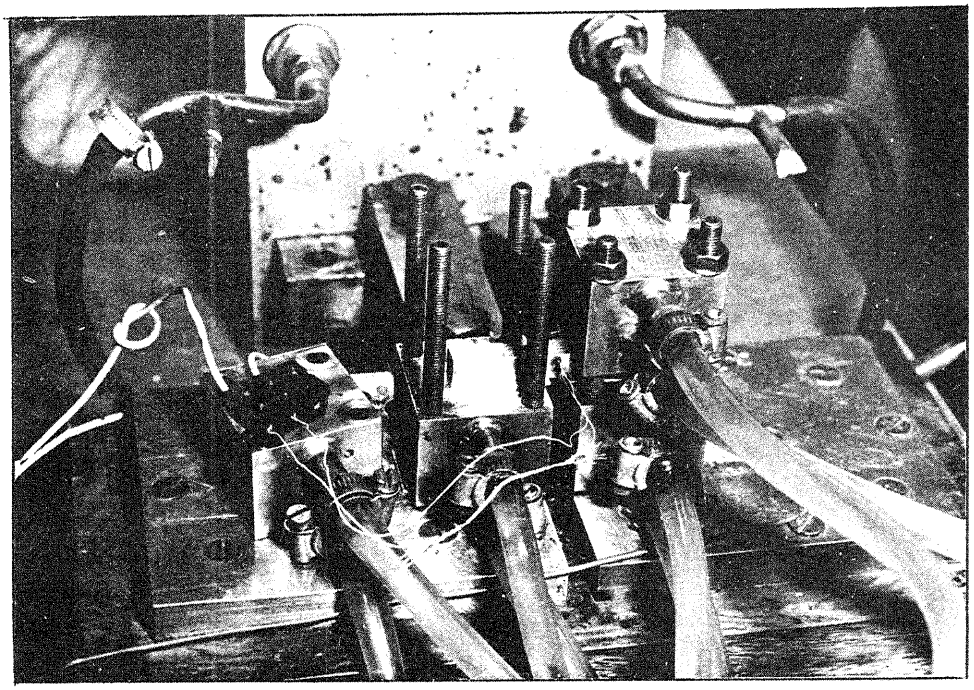

FIG. 4 SPECIMEN GRIP DESIGN AND THE POSITION OF THE FEEDBACK THERMOCOUPLE

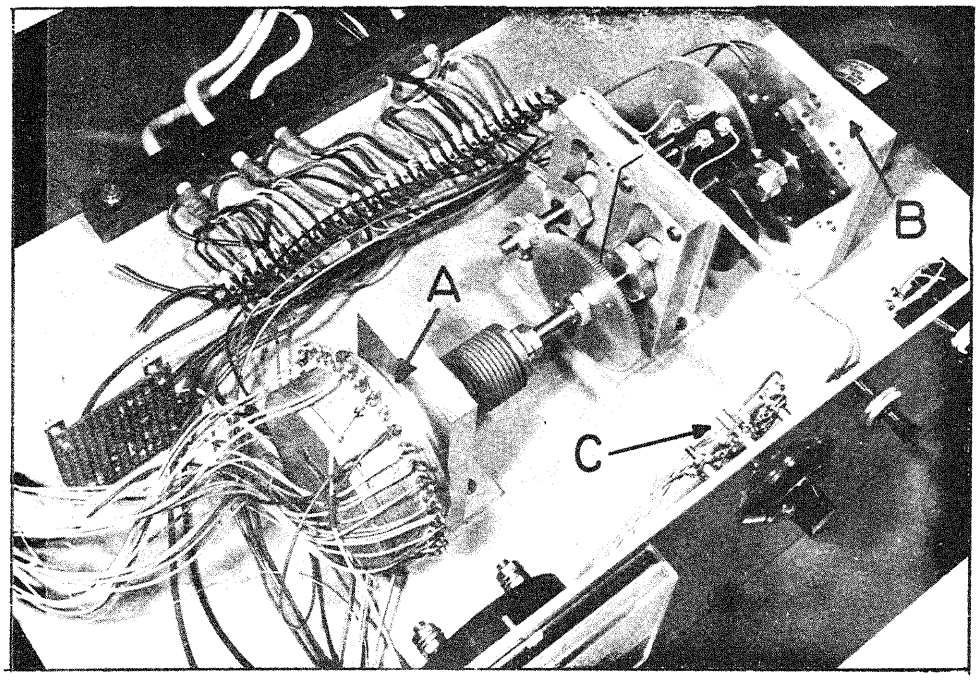

A - MULTI - TAP POTENTIOMETER.
B - SYNCHRONOUS MOTOR.
C - PEAK - POSITION SELECTOR SWITCH.

FIG. 5. - DETAILS OF THE FUNCTION GENERATOR.

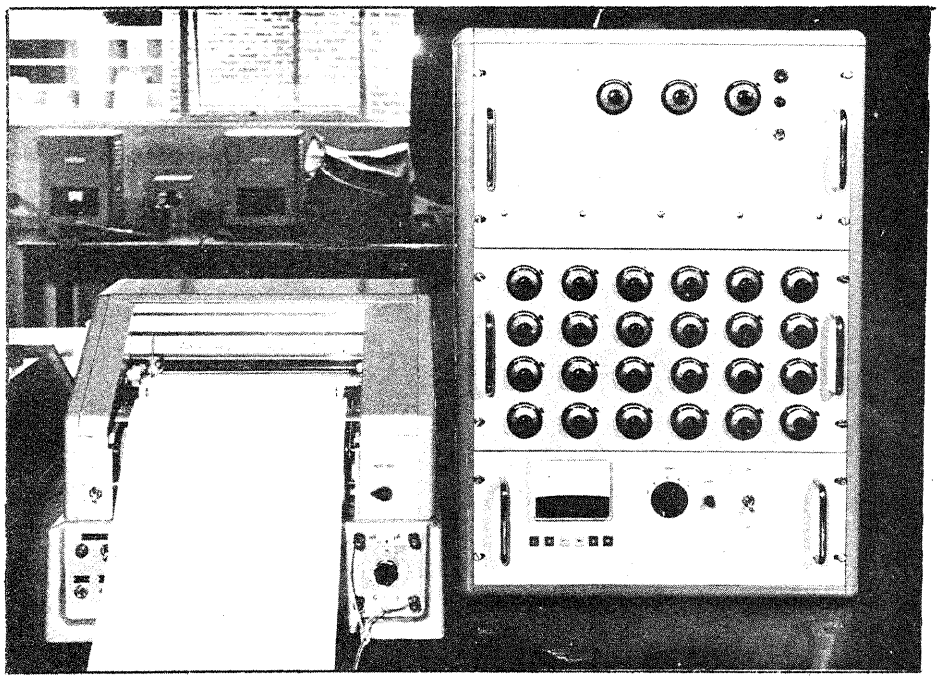

FIG. 6. GRAPHISPOT CHART RECORDER AND FUNCTION GENERATOR.

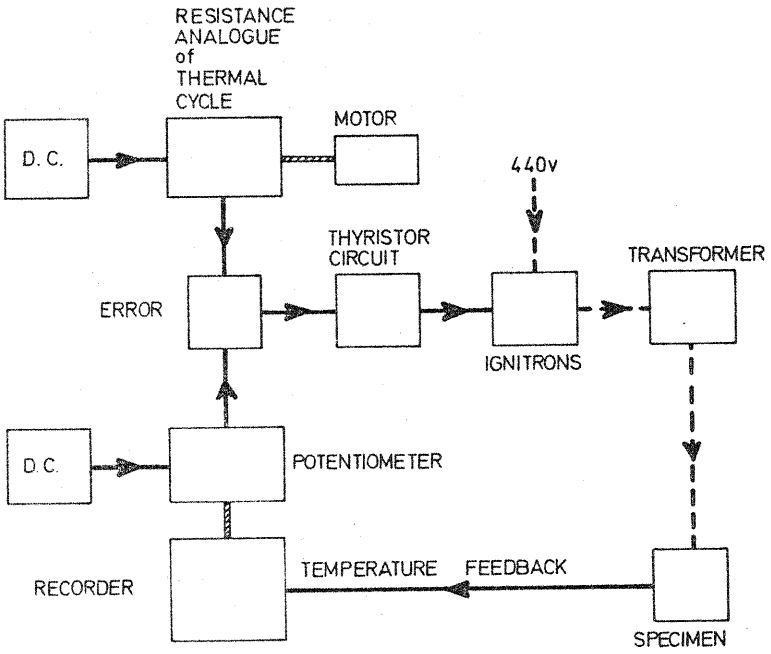

FIG. 7. SCHEMATIC DIAGRAM OF SIMULATOR.

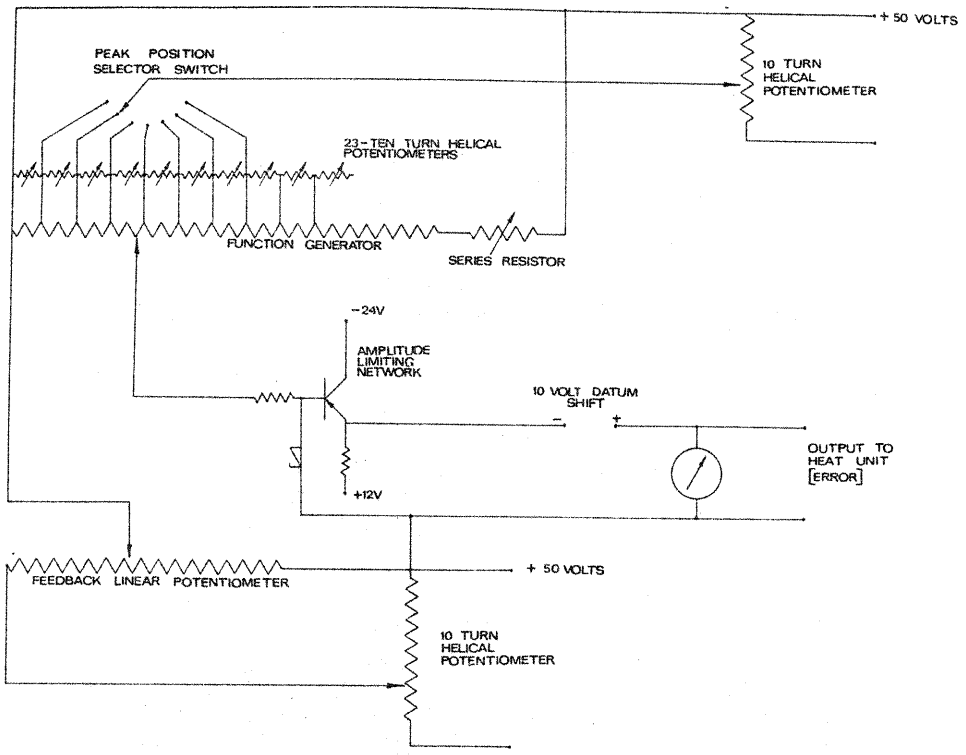

FIG. 8. CIRCUIT DIAGRAM OF SIMULATOR.

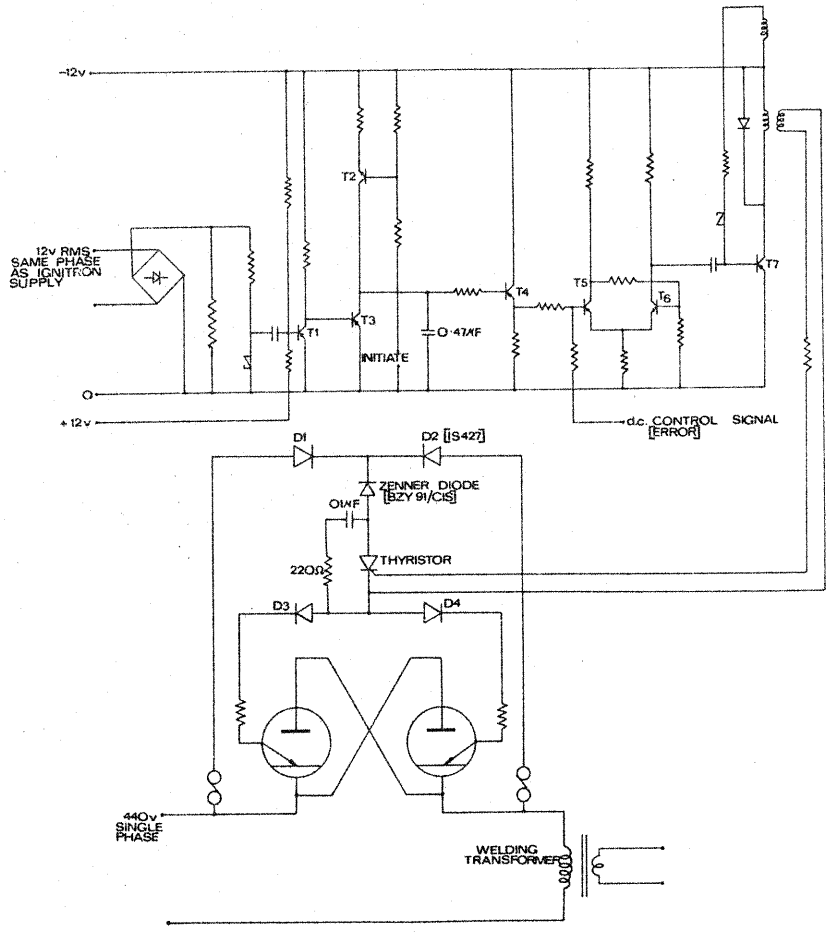

FIG. 9. CIRCUIT DIAGRAM OF HEAT CONTROL UNIT.

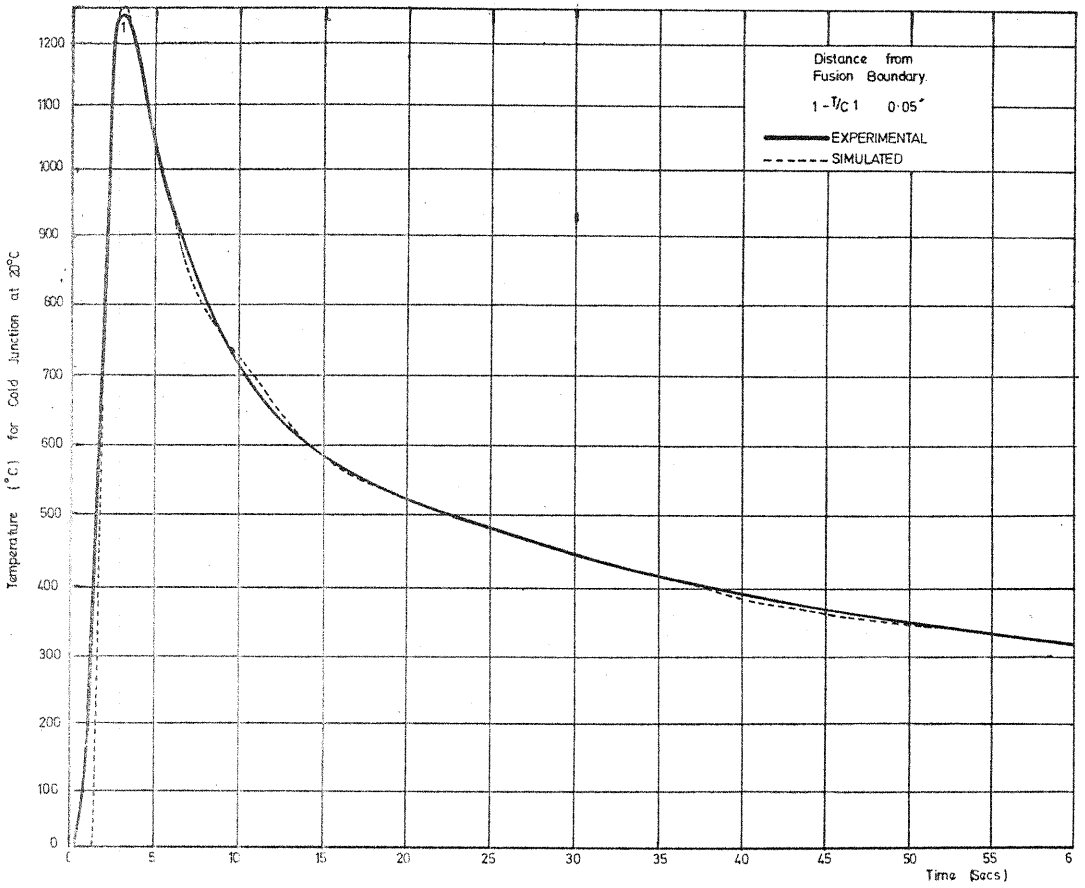

FIG. 10. COMPARISON OF EXPERIMENTAL AND SIMULATED CYCLES.

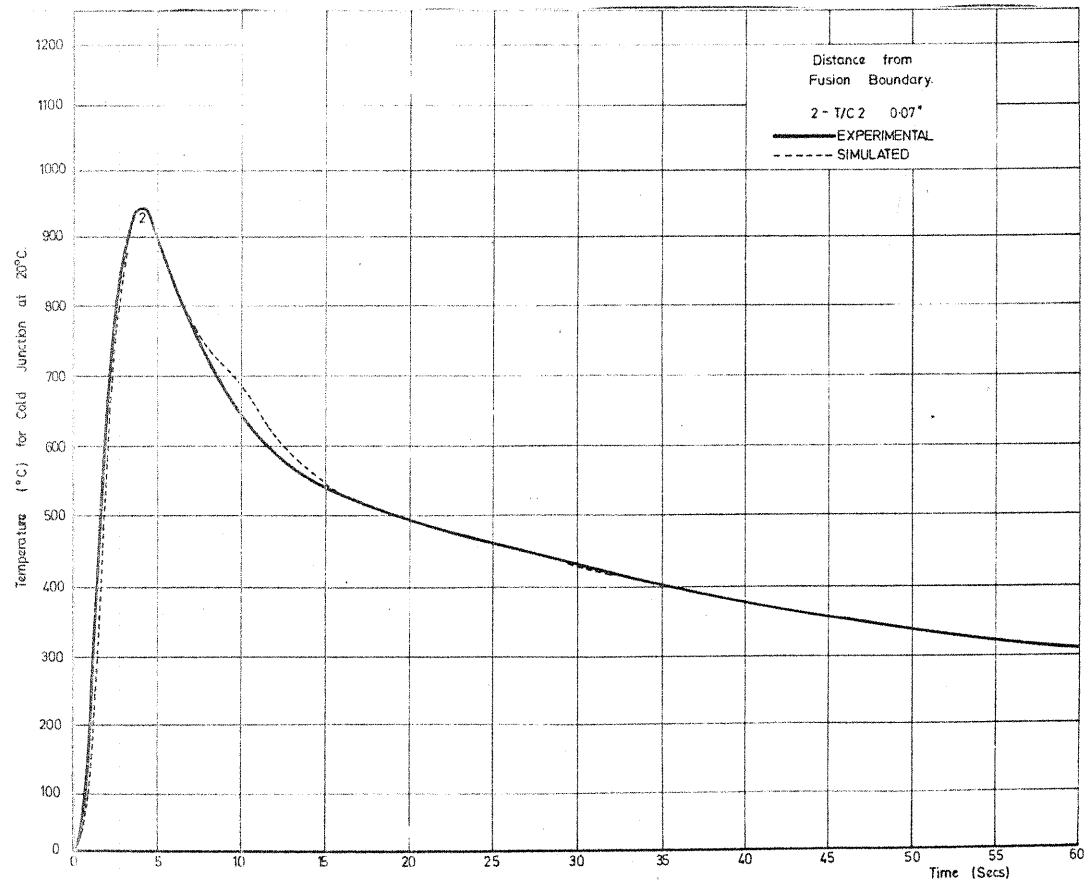

FIG. 11. COMPARISON OF EXPERIMENTAL AND SIMULATED CYCLES.

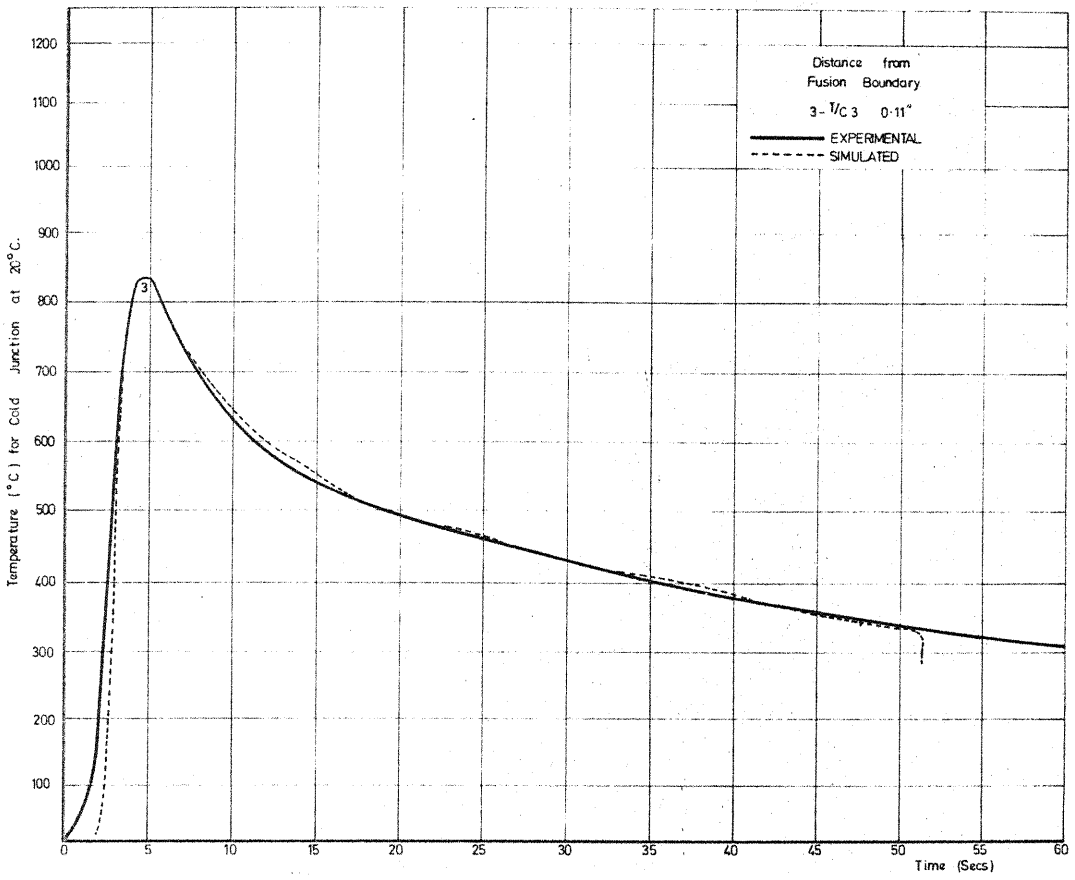

FIG. 12. COMPARISON OF EXPERIMENTAL AND SIMULATED CYCLES.

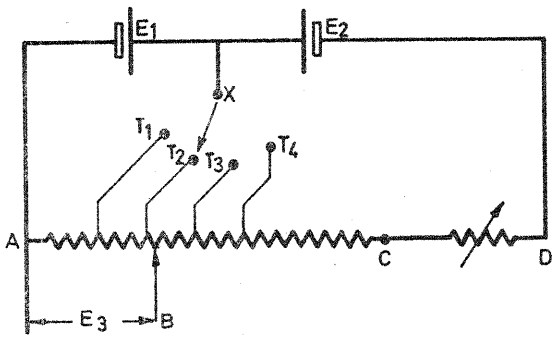

FIG. A 1.

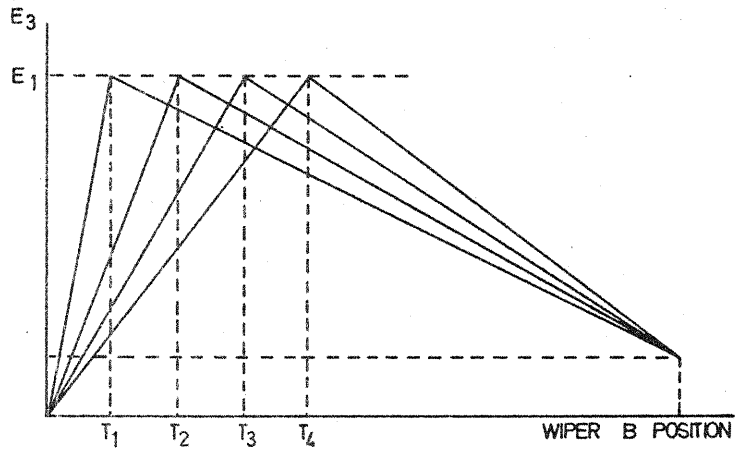

FIG. A 2.

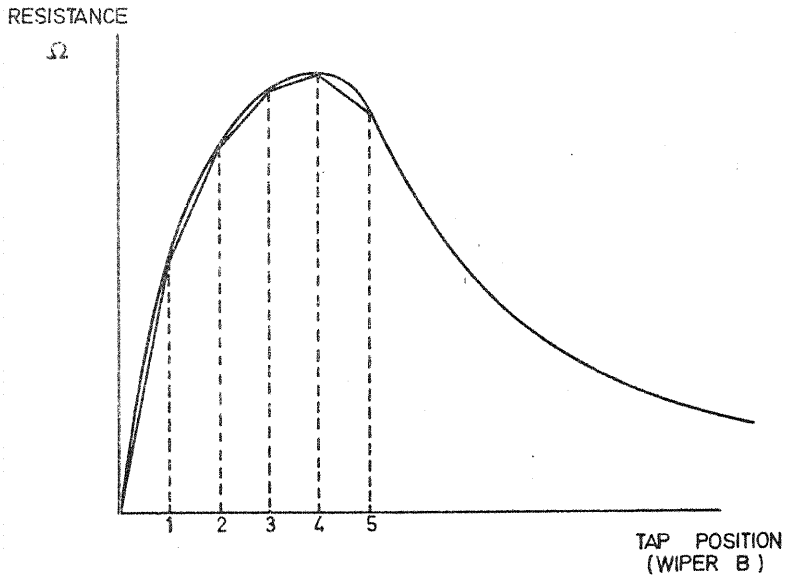

FIG. A 3.

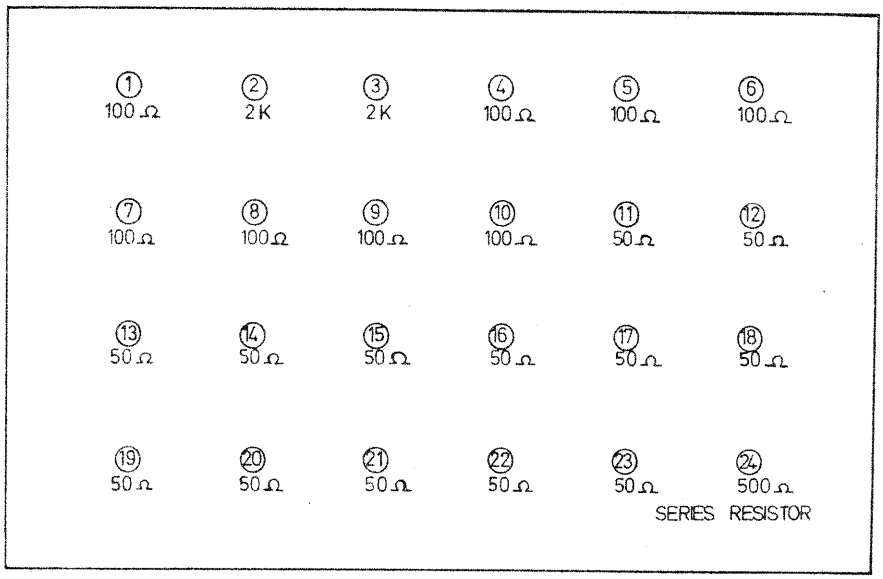

FIG. A6.

LAYOUT OF HELICAL POTENTIOMETERS

HELICAL POTENTIOMETER	VALUE Ω	TAPS
1	100	1 - 2
2	2000	2 - 3
3	2000	3 - 4
4	100	4 - 5
5	100	5 - 6
6	100	6 - 7
7	100	7 - 8
8	100	8 - 9
9	100	9 - 10
10	100	10 - 11
11	50	11 - 12
12	50	12 - 13
13	50	13 - 14
14	50	14 - 15
15	50	15 - 16
16	50	17 - 19
17	50	19 - 21
18	50	21 - 23
19	50	23 - 25
20	50	25 - 27
21	50	27 - 29
22	50	29 - 31
23	50	31 - 33
24	500	SERIES RESISTOR

FIG. A7 VALUES OF HELICAL POTENTIOMETERS AND THEIR TAP POSITIONS

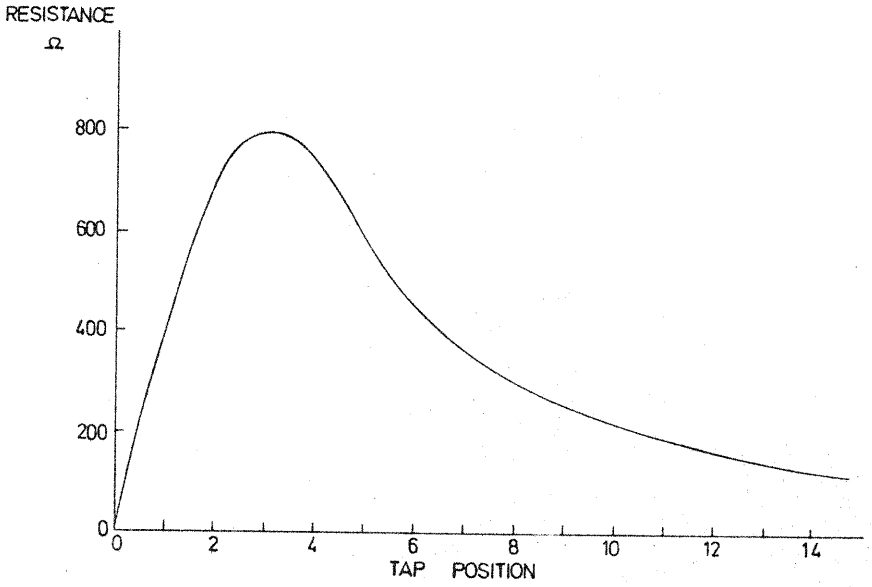
RESISTANCE
Ω
800
600
400
200
0
0
2
4
6
8
10
12
14
TAP POSITION

FIG. A 4.

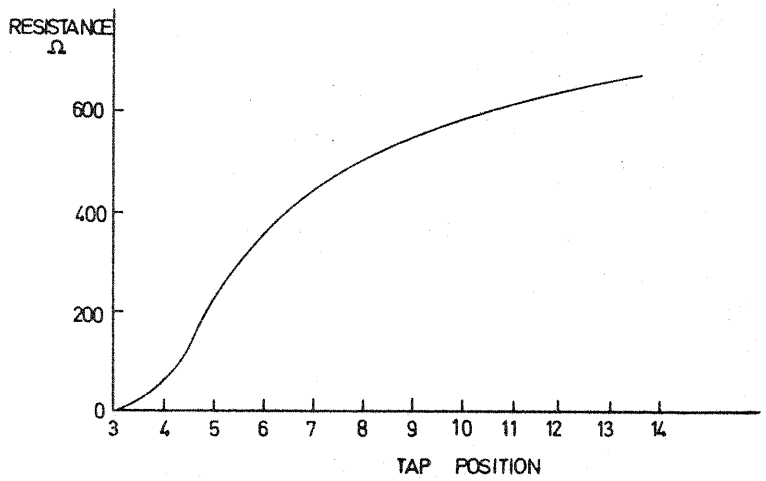
RESISTANCE
Ω
600
400
200
0
3
4
5
6
7
8
9
10
11
12
13
14
TAP POSITION

FIG. A 5.